



Executive Summary Report

Nano-Black Coating on Silicon CMOS Image Sensors for Extreme Sensitivity

for ESA contract 4000135291/21/NL/GLC/ov

Issue: 1

Revision: 0

Centre for Electronic Imaging

School of Physical Sciences
The Open University
Walton Hall
Milton Keynes, MK7 6AA
United Kingdom

		Date
Prepared by:	Martin Prest	08 June 2023
Checked by:	Konstantin Stefanov	08 June 2023
Document reference:	B-Si Executive Summary Report	

Document Change Record

Issue/ Revision	Date	Modified pages	Comments
<i>1.0</i>	<i>08 June 2023</i>		<i>Initial document</i>

Distribution List

OU Aalto Te2v ESA	Martin Prest, Konstantin Stefanov Olli Setala, Ville Vahanissi, Hele Savin Doug Jordan Matthew Soman
----------------------------	---

Contents

1	References.....	3
2	Abstract	4
3	Introduction.....	4
4	Experimental Results.....	5
4.1	QE measurements	5
4.2	Photoresponse non-uniformity (PRNU)	6
4.3	Dark Current.....	8
4.4	Modulation Transfer Function (MTF)	8
5	Summary & Conclusions.....	10

1 References

[1] M. Garin, J. Heinonen, L. Werner, T. P. Pasanen, V. Vähänissi, A. Haarahiltunen, M. A. Juntunen, and H. Savin, "Black-Silicon Ultraviolet Photodiodes Achieve External Quantum Efficiency above 130%", *Physical Review Letters* 125, 117702 (2020).

[2] Teledyne-e2v datasheet SIRIUS – CIS115 Back Illuminated CMOS Image Sensor [A1A-785580] Version 3, Feb 2019.

[3] C. Crews, M. Soman, E. A. Allanwood, K. Stefanov, M. Leese, P. Turner, and A. Holland "Quantum efficiency of the CIS115 in a radiation environment." *X-Ray, Optical, and Infrared Detectors for Astronomy IX*. Vol. 11454. 114540E International Society for Optics and Photonics, December 2020.

[4] *Electro-optical Test Methods for Charge Coupled Devices*, ESCC Basic Specification No. 25000, issue 2, January 2014.

[5] *CMOS Image Sensors*, K. D. Stefanov, ISBN 978-0-7503-3235-4, IOP Publishing (2022).

2 Abstract

A novel anti-reflection process was demonstrated which improves the quantum efficiency (QE) of a CMOS image sensor, with particular benefits at the ultraviolet (UV) and near infrared (NIR) ends of the electromagnetic spectrum. Also, the dark current and photoresponse non-uniformity (PRNU) were reduced to about 33% and 55%, respectively, of the values for a conventional control sensor. Spatial resolution seemed to be reduced in the NIR, as indicated by MTF measurements, but further investigations are required. The nano-black anti-reflection layer was made using a reactive-ion-etch technique to form nano-scale spikes at the surface which greatly reduce the reflectivity of the surface, which has a matt-black appearance. The sensor used, a CIS115 from Teledyne-e2v (as used for the JUICE JANUS camera), is a back-side-illuminated (BSI) device with $\approx 10 \mu\text{m}$ active silicon thickness and 2000×1504 pinned photodiode pixels with a pitch of $7 \mu\text{m}$. The improved QE is most impressive below 400 nm, where the QE increases towards 100%, although no correction was made for the increased quantum yield, as this is not easily quantified. The QE of a CIS115 sensor with a conventional antireflection (AR) coating shows a steep drop below 400 nm. There is also an improvement in QE in the NIR (from 700 nm to 1100 nm) for the nano-black sensor, and this is despite the approx. $1 \mu\text{m}$ thinning of the silicon by the etching process, which would normally reduce the QE. Some of the QE improvement may be the result of increased scattering of the incident light or by the improved surface passivation in the nano-black devices.

3 Introduction

Silicon image sensors are prone to poor QE at UV wavelengths because conventional surface passivation tends to cause a non-photoresponsive layer at the surface, which can be thicker than the absorption depth (only a few nm). Whereas at NIR wavelengths, the absorption depth required is 10s to 100s of μm , so thick layers are required. The sensor used in this work has an absorber of $10 \mu\text{m}$ thickness which is a compromise centred on visible wavelengths and for providing high spatial resolution. An anti-reflection process which improves QE at both ends of the visible spectrum would enable more applications for conventional CMOS sensors, which are the world's widest used image sensor technology.

The back-side passivation of the nanostructure uses an alumina (Al_2O_3) layer of 20 nm thickness deposited by atomic layer deposition (ALD). This layer chemically passivates dangling bonds at the surface and extrinsically induces a field in the silicon due to its fixed negative charge. This type of passivation eliminates the non-photoresponsive surface layer and has lower interface state density at the surface of the silicon compared to conventional image sensors which use a back-side implant for passivation, which may explain the lower dark current and increased QE at UV.

The nano-black process has previously demonstrated high QE in discreet photodiodes [1]. To the authors' knowledge, this is the first time that such a process has been applied to a monolithic CMOS image sensor. The nano-black anti-reflection layer was fabricated without modifying the standard BSI process, as a last step, in place of applying an AR coating. The nano-black fabrication process is a low-temperature ($\sim 120 \text{ }^\circ\text{C}$) reactive-ion plasma etch which produces a nano-structured surface of closely spaced spikes with average height 500 nm and width 100 nm. This surface then receives a conformal coating of 20 nm Al_2O_3 , deposited by atomic layer deposition, with negative surface charge to provide a field-effect passivation. Fig. 1a shows an electron micrograph of the nano-structured silicon surface. The spiked shapes cause multiple reflections between the structures trapping the light to reduce reflectivity; or is alternatively explained as a gradual change in refractive index as light approaches the surface. Fig. 1b shows a CIS115 [2] sensor with nano-black layer covering the lower half of the pixel array.

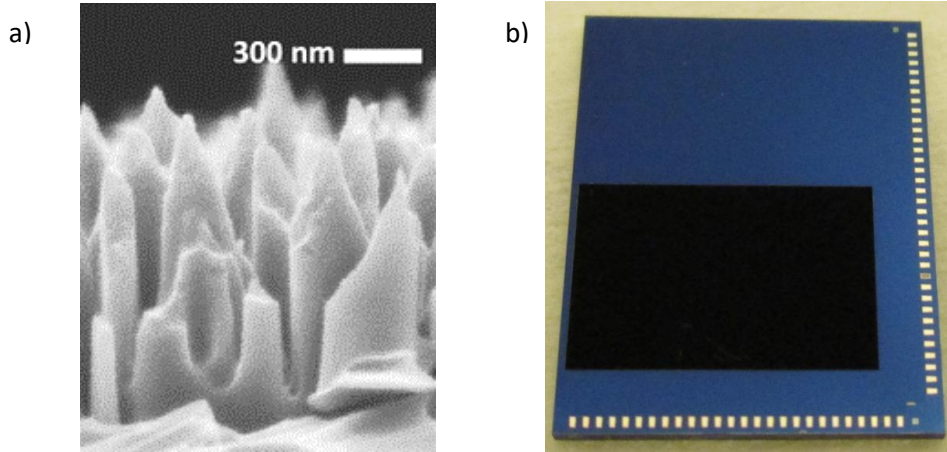


Figure 1. (a) electron micrograph of the nano-black surface, reproduced from [1], (b) nano-black layer on lower half of a CIS115 sensor

4 Experimental Results

During all measurements, the sensors were mounted in a vacuum chamber, and the temperature was controlled to 20 °C with a stability within ± 0.05 °C, using a water-cooled thermoelectric cooler (TEC).

4.1 QE measurements

Quantum efficiency (QE) is the percentage ratio of the number of photogenerated electrons N_e measured for a given number of incident photons N_p of specified wavelength λ :

$$QE(\lambda) = \frac{N_e(\lambda)}{N_p(\lambda)} \times 100\%. \quad (1)$$

QE measurements were taken in the wavelength range 300 nm to 1100 nm, in 20 nm steps, using a method previously developed for the Juice JANUS camera [3]. A nano-black sensor is compared to the AR coated control in Fig. 2. The experimental error in the QE results is about 4%, as indicated by error bars for the control sensor (error bars are not shown for the nano-black sensor to aid clarity). The nano-black QE results are higher across most of the wavelength range, but the increase in QE is greatest at the UV end of the spectrum, because for the AR coated sensor the QE drops sharply for wavelengths below 400 nm. QEs greater than 100% are a result of quantum yield higher than unity, i.e., more than one electron generated per photon which occurs for wavelengths below ≈ 330 nm.

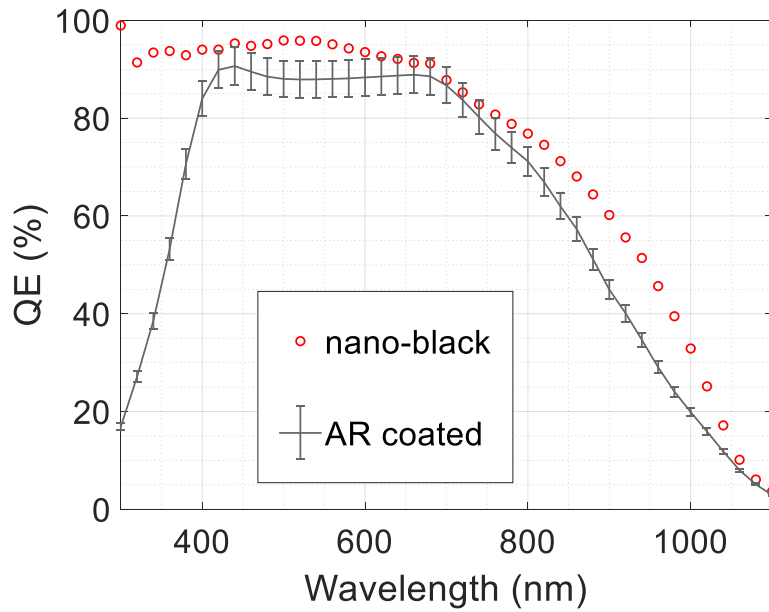


Figure 2. QE results, comparing a nano-black sensor (red circles) to the control AR coated sensor (gray curve with error bars).

4.2 Photoresponse non-uniformity (PRNU)

For the PRNU measurements, the optical setup was modified to obtain an improved flat-field illumination. The PRNU is a measure of how the signal varies across the pixel array for a flat-field illumination. In practice it is difficult to achieve perfectly flat-field illumination, so a local moving mean has been taken of the surrounding pixels in a 25×25 pixel square.

The $PRNU_{pix}$ contribution of each pixel was calculated according to [4] ignoring the first 4 rows and columns of the image area:

$$PRNU_{pix} = \frac{V_{si} - V_a}{V_a} \times 100\% \quad (2)$$

where V_{si} = individual pixel signal and V_a = local mean signal. The sensor PRNU was calculated from the standard deviation of a Gaussian fit to the $PRNU_{pix}$ histogram, to reject the non-gaussian data of defective pixels. The lit frames were taken in the linear range of operation, for an integration time of 0.7 s, corresponding to about 1/2 full well capacity.

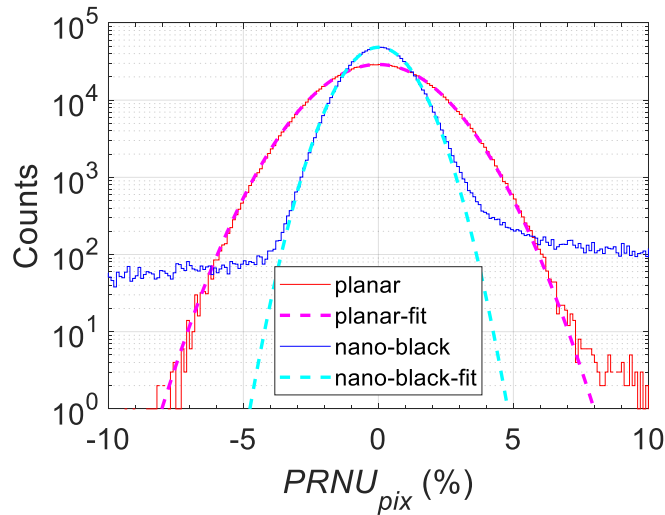


Figure 3. Histogram of $PRNU_{pix}$ for planar and nano-black regions of sensor with Gaussian fits using monochromatic illumination at a wavelength of 500 nm.

Measurements were taken using a sensor divided into two regions, with a nano-black surface for one half and the planar control BSI passivation (without AR coating) for the other half of the chip. The $PRNU_{pix}$ for the two regions is shown using histograms in Fig. 3. The standard deviation of the Gaussian fits, giving the sensor PRNU, were 1.0% for the nano-black region and 1.8% for the planar region. The nano-black histogram has higher shoulders (at a count of around 100) where the distribution becomes non-Gaussian because of a scratch in the surface causing more defective pixels (this scratch can be seen in the dark current pixel map of Fig. 5).

The sensor PRNU was also measured for varying wavelength as shown in Fig. 4. The PRNU is lower at all wavelengths for the nano-black region of the chip, compared to the planar region. PRNU is highest for both regions at the shortest wavelengths. The PRNU is less wavelength dependent for the nano-black which perhaps shows that scattering is not likely to be the reason for the lower PRNU because scattered light might be expected to have a stronger wavelength dependence.

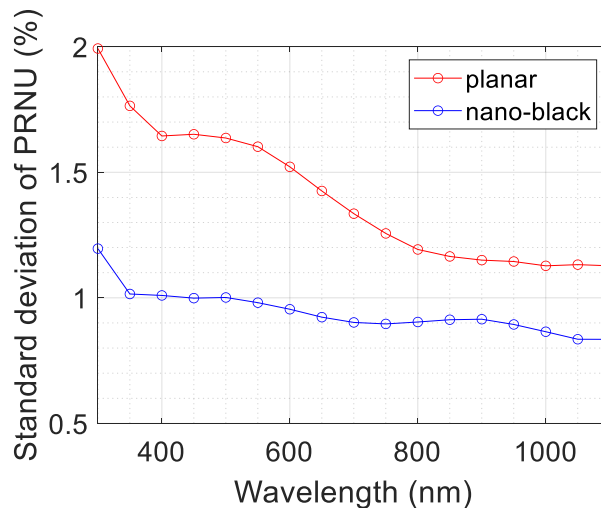


Figure 4. PRNU versus wavelength for sensor, showing comparison of the planar and nano-black regions.

4.3 Dark Current

The dark current was measured at 20 °C using a sensor which had half of its surface with the nano-black process, the other half had a planar surface with the control BSI passivation consisting of a shallow boron implant and anneal, but no AR coating. Fig. 5a shows a pixel map of the dark current for the sensor. In Fig. 5b, the histogram of pixel signals from the sensor has 2 peaks, at 9 and 27 e⁻/pix/s for the nano-black and planar regions, respectively. These results show that the nano-black region clearly has lower dark current than the planar region.

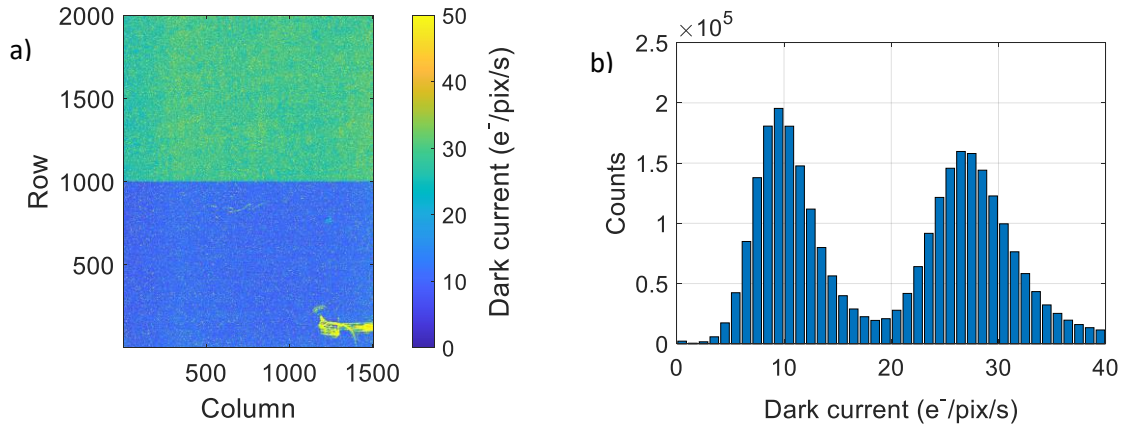


Figure 5. (a) Dark current pixel map of sensor at 20 °C. Upper half: planar; lower half: nano-black. (b) Dark current histogram of full pixel array, showing the nano-black region (left peak) and the planar region (right peak).

4.4 Modulation Transfer Function (MTF)

The modulation transfer function (MTF) is a measure of the spatial resolution. It was measured using the slanted edge method [5], where a metal mask is directly deposited onto the image sensor surface. In Figure 6 the MTF at a normalised spatial frequency of 0.5 (the Nyquist frequency) has been calculated as a function of wavelength for the nano-black chips. The MTF drops off at longer wavelengths with a peak at around 500 nm, with a slight drop at shorter wavelengths. The drop in MTF at longer wavelengths may be related to the slight reduction of PRNU at longer wavelengths; increased scattering of light at longer wavelengths could smooth-out non-uniformities between pixels. For comparison, MTF measurements performed on a CIS115 for the JUICE project are shown in Figure 7. The JUICE measurements used a different method both at Te2v and the OU (projection of light slit line spread function, rather than using the mask method), which may or may not account for the absolute difference in MTF value between the datasets, however, it's clear that the conventional CIS115s of the JANUS camera do not show a drop in MTF at longer wavelengths.

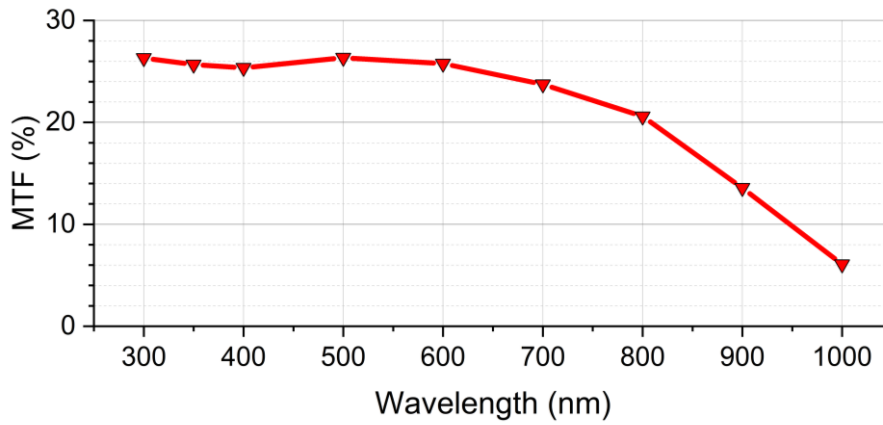


Figure 6. MTF at Nyquist vs. wavelength for nano-black chips.

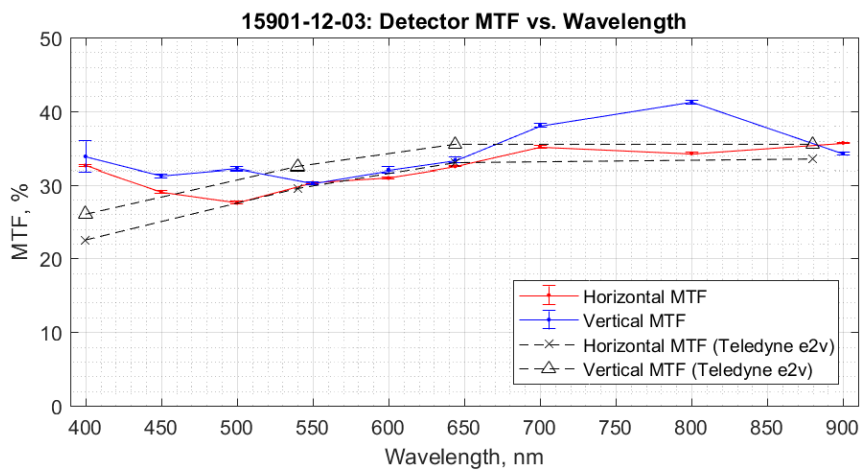


Figure 7. MTF measurements performed for the JUICE JANUS camera at the OU (red and blue lines), and measurements performed at Te2v (black dashed lines).

5 Summary & Conclusions

A nanostructured anti-reflection surface (black-silicon) was applied to a conventional CMOS image sensor, showing improvement in QE over the spectral range from 300 nm to 1000 nm. Such nanostructures are attracting increased interest for solar cells and photodiodes, where significant performance gains have been demonstrated. For image sensors, the parameters of spatial resolution, uniformity and high dynamic range are of additional interest, and are investigated in this work; uniformity was increased, but spatial resolution was degraded. Dark current was reduced to 1/3, which could result in either increased dynamic range or higher operating temperature.

The increase in QE of the black-silicon sensors is mainly the result of reduced reflectivity over a wide wavelength range, but also the improved passivation. The high QE at short wavelengths is consistent with results for discreet nano-black photodiodes [1] and is attributed to a combination of low reflectivity, good absorption and a quantum yield greater than one, i.e., more than one electron produced per photon. The control CIS115's AR coating was not UV optimised, which contributes to its sharp cut-off in QE below 400 nm. Also, its conventional back surface passivation reduces QE in the UV because it causes a non-photoresponsive surface layer of a few nm thickness. In contrast, the thin Al₂O₃ passivation of the nano-black devices allows absorption within those first few nm of the silicon because of its extrinsic field-passivation.

For high QE in the NIR, a relatively thick silicon absorber is required. The CIS115 is only 10 µm thick (which is approximately equal to the absorption length at 800 nm wavelength) and explains the drop-off in QE beyond 700 nm. The relative improvement in QE in the NIR for the nano-black sensor is despite the approximate 1 µm thinning of the silicon by the nano-black etching process, which would normally reduce the QE. However, some of this improvement may be attributed to increased light scattering, as indicated by the reduced PRNU.

Dark current and PRNU were reduced in nano-black sensors compared to a conventional planar BSI control. Dark current was 33% of that for the planar control. PRNU was 55% of that for the planar control. The dark current improvement could be related to the improved surface passivation.

We believe that the low PRNU of the nano-black surface compared to the planar surface is either indicative of increased scattering of light, which could smooth-out non-uniformities between pixels, or is perhaps the result of the improved passivation, which may better explain the PRNU reduction for wavelengths up to 500 nm, for which the absorption depth is shallower and more susceptible to non-uniformities in the passivation. The higher QE of the nano-black surface, particularly at longer wavelengths where the QE improvement is more modest, could also be related to the reduced PRNU because scattering could result in an increased probability of light transmission or a longer optical path length. The QE gain at longer wavelengths is associated with a decrease in spatial resolution as shown by the MTF results, which may also be the result of increased scattering. This degradation in MTF could possibly be mitigated in future sensors using deep trench isolation.

In this work it was shown, for first time, that the nano-black process can be used in place of conventional AR coatings for CMOS image sensors, and can be performed as a final step after CMOS fabrication and back-thinning. The commercial viability of the nano-black process depends upon addressing concerns about the ability to clean a non-planar surface and difficulties in handling during packaging, but the improved QE and reduced dark current are good reasons to further pursue this technology.